JOC Article

Claisen Rearrangement of Aliphatic Allyl Vinyl Ethers in the Presence of Copper(II) Bisoxazoline

Bülent Balta,*,† Cem Öztürk,‡ Viktorya Aviyente,*,‡ Mark A. Vincent,§ and Ian H. Hillier§

Polymer Research Center and Department of Chemistry, Boğaziçi University, 34342, Bebek, Istanbul, Turkey, and School of Chemistry, University of Manchester, Oxford Road, Manchester M13 9PL, U.K.

baltbule@yahoo.com; aviye@boun.edu.tr

Received January 15, 2008

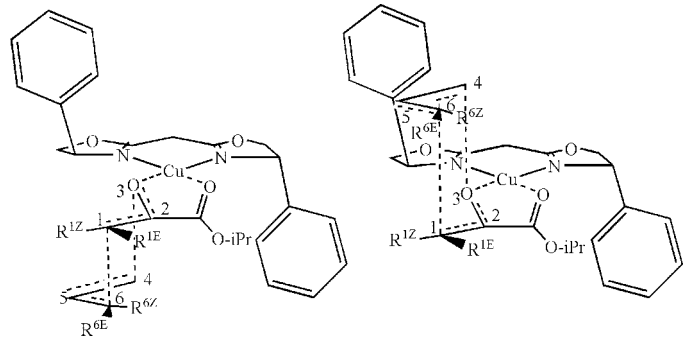

The Claisen rearrangement of 1-methyl-2-isopropyoxycarbonyl-6-propyl allyl vinyl ether catalyzed by copper(II) bisoxazoline (Cu-box) has been investigated using density functional theory. Both the phenyl- and *tert*-butyl-substituted Cu-box systems have been studied. Three different reaction media (vacuum, CH_2Cl_2, CH_3CN) have been considered. In vacuum, the phenyl Cu-box catalyzed reaction yields a (1*R*,6*R*) configured major product with a low selectivity. The solvent induces a higher selectivity and a reversal of the absolute configuration (1*S*,6*S*). However, the *tert*-butyl Cu-box catalyzed reaction yields (1*R*,6*R*) as the major product both in the gas phase and in the solvent with a good selectivity. Although chair-like TSs are lower in energy than boat-like TSs, the energy difference is small. This is because in the presence of the catalyst the distance between the allyl and vinyl parts of the substrate is relatively large, and thus the steric repulsion between them is smaller than would normally be expected for boat-like structures. The enantioselectivity of *tert*-butyl Cu-box originates from the steric interactions between the substrate and the catalyst, which are less important for the phenyl Cu-box where the enantioselectivity is determined by the solvent effects.

Introduction

The Claisen rearrangement, the [3,3]-sigmatropic rearrangement of allyl vinyl ethers, is a synthetically important reaction because it converts a C−O single bond to a C−C single bond, creating two new stereocenters.[1] The reaction has an inherent diastereoselectivity, explained by the preference for chair-like transition states (TSs) over boat-like ones (note, however, that boat-like TSs were found to be more favorable in some Ireland−Claisen rearrangements due to the steric effects).[2] 1-Methyl-2-isopropyoxycarbonyl-6-propyl allyl vinyl ether **1** rearranges to **2** as a single diastereomer (Scheme 1).[3] However, this reaction is not enantioselective, a racemic mixture of (1*R*,6*S*)-**2** and (1*S*,6*R*)-**2** being obtained through two possible chair-like TSs (Scheme 1). The reaction is completed in 24 h at 100 °C in $ClCH_2CH_2Cl$ with 99% yield.[3]

The Claisen rearrangement TSs are early with the C−O bond breaking being more advanced than the formation of the new C−C bond.[1,4–7] The TSs are thought to have dipolar nature,

† Polymer Research Center, Boğaziçi University.
‡ Department of Chemistry, Boğaziçi University.
§ University of Manchester.

(1) Martin Castro, A. M. *Chem. Rev.* **2004**, *104* (6), 2939–3002.
(2) Khaledy, M. M.; Kalani, M. Y. S.; Khuong, K. S.; Houk, K. N.; Aviyente, V.; Neier, R.; Soldermann, N.; Velker, J. *J. Org. Chem.* **2003**, *68* (2), 572–577.
(3) Hiersemann, M.; Abraham, L. *Eur. J.Org. Chem.* **2002**, *2002* (9), 1461–1471.
(4) Vance, R. L.; Rondan, N. G.; Houk, K. N.; Jensen, F.; Borden, W. T.; Komomicki, A.; Wimmer, E. *J. Am. Chem. Soc.* **1988**, *110* (7), 2314–2315.
(5) Gajewski, J. J. *Acc. Chem. Res.* **1997**, *30* (5), 219–225.
(6) Aviyente, V.; Yoo, H. Y.; Houk, K. N. *J. Org. Chem.* **1997**, *62* (18), 6121–6128.

10.1021/jo800101g CCC: $40.75 © 2008 American Chemical Society
Published on Web 06/11/2008

SCHEME 1. Thermal Claisen rearrangement of Aliphatic Allyl Vinyl Ether 1

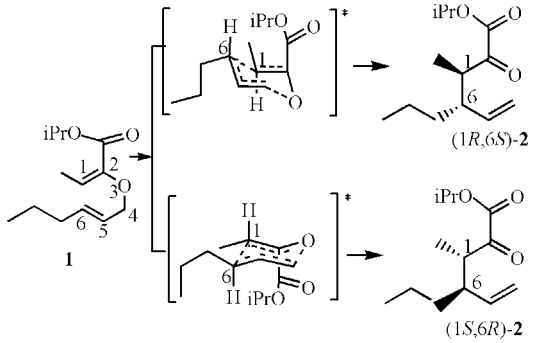

consisting of an enolate-like moiety and an allylic cation-like moiety.[1,6,8] However, some kinetic isotope effect measurements argue against the involvement of an ionic TS.[5,9] Hartree−Fock (HF) and density functional theory (DFT) calculations predict a more ionic TS than does the CASSCF method, which indicates a wave function with biradical character.[10,11] On the other hand, according to experiments, the presence of an ion pair as a stable intermediate is unlikely.[8] Polar solvents were found to enhance the reaction rate.[1,5,8] Computational studies suggest that the rate acceleration in water originates from the electrostatic solvation effects and electronic polarization of the solute.[12–18] Hydrophobic effects were computed to be smaller.[12,13,16] In addition, hydrogen bonding to the ether oxygen was found to be stronger in the TS than in the ground state.[15,16,19]

A number of Lewis acids such as Sc^{III}, Yb^{III}, and Cu^{II} catalyze Claisen rearrangements.[1,3,20] The Lewis acid was thought to coordinate to the ether O, to destabilize the breaking O−C bond and to stabilize the developing negative charge on the oxygen atom of the enolate-like moiety. None of the experimentally studied Lewis acid catalyzed reactions was enantioselective.

The C_2 symmetric catalyst Cu^{II} bisoxazoline (Cu-box)[21–24] was used to combine the inherent diastereoselectivity of the Claisen rearrangement with a good level of enantioselectivity.[3,25–29] The two most commonly used Cu-box catalysts have *tert*-butyl or phenyl groups as substituents with triflate (OTf^-) or SbF_6^- employed as counterions (Scheme 2).

SCHEME 2. (*S*,*S*)-Cu-box

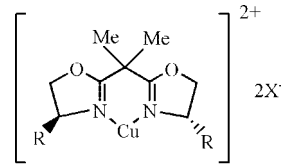

3a: R=t-butyl, X=OTf^-
3b: R=t-butyl, X=SbF_6^-
3c: R=phenyl, X=OTf^-
3d: R=phenyl, X=SbF_6^-

Some experimental results by Hiersemann and co-workers are summarized in Scheme 3.[3,25,27] Z-Configured allyl groups give very good diastereoselectivities and enantioselectivities. On the other hand, E-configured allyl groups give lower diastereoselectivities, and in some cases, unexpected diastereomers (thought to arise from boat-like TSs) are observed (Scheme 3, entries 9, 15). Catalysts **3b** and **3c** give the opposite enantiomers as major products. The sterically more demanding catalyst **3b** is more enantioselective. (*R*,*R*)-Configured catalysts yield the opposite enantiomer with respect to (*S*,*S*)-configured ones (not shown).

Scheme 4 displays the proposed chair-like TS for the Claisen rearrangement catalyzed by **3b**.[3,25,27] The ether O and the carbonyl O of the alkoxycarbonyl substituent at C2 chelate the copper atom in a square planar geometry. The allylic moiety is expected to be mostly situated at the unhindered side of the vinyl group, resulting in enantioselectivity.

X-ray crystallography showed that ligands around the *tert*-butyl Cu-box are positioned as in Scheme 5 (counterions and hydrogens omitted).[21,23,30] The space around the catalyst is divided into four quadrants for ease of discussion. The *tert*-butyl substituents occupy regions A and C, whereas the ligands are situated in regions B and D, probably because of steric interactions. On the other hand, ligands around the phenyl Cu-box can be positioned as in either Scheme 5 or Scheme 6 (hereafter called type I and type II arrangements, respectively).[23] In the latter case, ligands are situated in quadrants A and C already occupied by the phenyl groups. When the ligands are Br^-, a type I arrangement is observed, while a type II pattern is seen for water.[23] Upon complexation with a 2-alkoxycarbonyl-substituted allyl vinyl ether, the ligands seen in the crystal structures are replaced by the oxygen atoms of the substrate chelating to the Cu.

Cu-box has also been used as a stereoselective catalyst for several related reactions, such as cyclopropanation, aziridination, aldol, Diels−Alder, and carbonyl-ene reactions.[21–24] In Diels−Alder reactions, Jørgensen and co-workers observed that the selectivity of the phenyl-substituted Cu-box changed with the solvent polarity, whereas the *tert*-butyl-substituted catalyst did

(7) Meyer, M. P.; DelMonte, A. J.; Singleton, D. A. *J. Am. Chem. Soc.* **1999**, *121* (47), 10865–10874.
(8) Coates, R. M.; Rogers, B. D.; Hobbs, S. J.; Peck, D. R.; Curran, D. P. *J. Am. Chem. Soc.* **1987**, *109* (4), 1160–1170.
(9) Gajewski, J. J.; Brichford, N. L. *J. Am. Chem. Soc.* **1994**, *116* (7), 3165–3166.
(10) Wiest, O.; Black, K. A.; Houk, K. N. *J. Am. Chem. Soc.* **1994**, *116* (22), 10336–10337.
(11) Yoo, H. Y.; Houk, K. N. *J. Am. Chem. Soc.* **1994**, *116* (26), 12047–12048.
(12) Cramer, C. J.; Truhlar, D. G. *J. Am. Chem. Soc.* **1992**, *114* (23), 8794–8799.
(13) Davidson, M. M.; Hillier, I. H.; Hall, R. J.; Burton, N. A. *J. Am. Chem. Soc.* **1994**, *116* (20), 9294–9297.
(14) Hall, R. J.; Davidson, M. M.; Burton, N. A.; Hillier, I. H. *J. Phys. Chem.* **1995**, *99* (3), 921–924.
(15) Guest, J. M.; Craw, J. S.; Vincent, M. A.; Hillier, I. H. *J. Chem. Soc., Perkin Trans. 2* **1997**, *1997* (1), 71–74.
(16) Davidson, M. M.; Hillier, I. H. *J. Phys. Chem.* **1995**, *99* (17), 6748–6751.
(17) Gao, J. *J. Am. Chem. Soc.* **1994**, *116* (4), 1563–1564.
(18) Sehgal, A.; Shao, L.; Gao, J. *J. Am. Chem. Soc.* **1995**, *117* (45), 11337–11340.
(19) Severance, D. L.; Jorgensen, W. L. *J. Am. Chem. Soc.* **1992**, *114* (27), 10966–10968.
(20) Hiersemann, M.; Abraham, L. *Org. Lett.* **2001**, *3* (1), 49–52.
(21) Johnson, J. S.; Evans, D. A. *Acc. Chem. Res.* **2000**, *33* (6), 325–335.
(22) Evans, D. A.; Rovis, T.; Johnson, J. S. *Pure Appl. Chem.* **1999**, *71* (8), 1407–1415.
(23) Desimoni, G.; Faita, G.; Jørgensen, K. A. *Chem. Rev.* **2006**, *106* (9), 3561–3651.
(24) Ghosh, A. K.; Mathivanan, P.; Cappiello, J. *Tetrahedron: Asymmetry* **1998**, *9* (1), 1–45.
(25) Abraham, L.; Czerwonka, R.; Hiersemann, M. *Angew. Chem., Int. Ed.* **2001**, *40* (24), 4700–4703.
(26) Helmboldt, H.; Hiersemann, M. *Tetrahedron* **2003**, *59* (23), 4031–4038.
(27) Abraham, L.; Körner, M.; Schwab, P.; Hiersemann, M. *Adv. Synth. Catal.* **2004**, *346* (11), 1281–1294.
(28) Abraham, L.; Körner, M.; Hiersemann, M. *Tetrahedron Lett.* **2004**, *45* (18), 3647–3650.
(29) Körner, M.; Hiersemann, M. *Synlett* **2006**, *2006* (1), 121–123.
(30) Evans, D. A.; Johnson, J. S.; Burgey, C. S.; Campos, K. R. *Tetrahedron Lett.* **1999**, *40* (15), 2879–2882.

SCHEME 3. Experimental Results by Hiersemann and Co-workers[3,25,27] on Various Claisen Rearrangements[a]

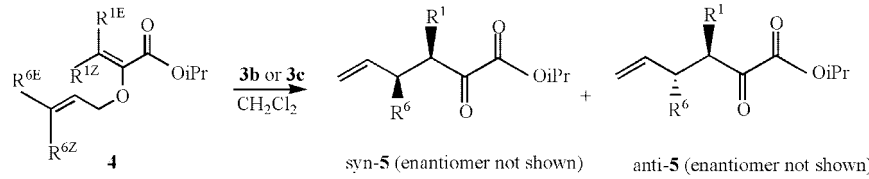

Substituents	catalyst	time (h)	syn/anti	ee%	absolute configuration
R^{1E} = methyl, R^{6E} = n-propyl : E,E-**4a**	**3c**	12	86/14	82	(1*S*,6*R*)
R^{1Z} = methyl, R^{6E} = n-propyl : Z,E-**4a**	**3c**	4	28/72	72	(1*R*,6*R*)
R^{1E} = methyl, R^{6Z} = n-propyl : E,Z-**4a**	**3b**	3	3/97	98	(1*R*,6*R*)
R^{1E} = methyl, R^{6Z} = n-propyl : E,Z-**4a**	**3c**	38	3/97	88	(1*S*,6*S*)
R^{1Z} = methyl, R^{6Z} = n-propyl : Z,Z-**4a**	**3b**	3	99/1	99	(1*S*,6*R*)
R^{1Z} = methyl, R^{6Z} = n-propyl : Z,Z-**4a**	**3c**	38	99/1	84	(1*R*,6*S*)
R^{1Z} = benzyl, R^{6E} = n-propyl : Z,E-**4b**	**3c**	6	44/56	n.d.	
R^{1Z} = benzyl, R^{6Z} = n-propyl : Z,Z-**4b**	**3c**	48	95/5	82	(1*R*,6*S*)
R^{1Z} = isopropyl, R^{6E} = n-propyl : Z,E-**4c**	**3c**	7	85/15	n.d.	
R^{1Z} = isopropyl, R^{6Z} = n-propyl : Z,Z-**4c**	**3c**	24	94/6	n.d.	
R^{1Z}= isopropenyl, R^{6Z} = n-propyl : Z,Z-**4d**	**3c**	24	92/8	86	(1*R*,6*S*)
R^{1E} = OBn, R^{6Z} = OBn : E,Z-**4e**	**3b**	24	1/99	99	(1*S*,6*R*)
R^{1Z} = OBn, R^{6Z} = OBn : Z,Z-**4e**	**3b**	12	99/1	99	(1*R*,6*R*)
R^{1E} = OBn, R^{6E} = OTPS : E,E-**4f**	**3b**	4	89/11	94	(1*S*,6*S*)
R^{1Z} = OBn, R^{6E} = OTPS : Z,E-**4f**	**3b**	4	63/37	99	(1*R*,6*R*)
R^{1E} = OBn, R^{6Z} = OTPS : E,Z-**4f**	**3b**	8	14/86	98	(1*S*,6*R*)
R^{1Z} = OBn, R^{6Z} = OTPS : Z,Z-**4f**	**3b**	3	99/1	98	(1*R*,6*R*)
R^{1E} = OTPS, R^{6Z} = OBn : E,Z-**4g**	**3b**	1.5	1/99	99	(1*S*,6*R*)
R^{1Z} = OTPS, R^{6Z} = OBn : Z,Z-**4g**	**3b**	1.5	99/1	99	(1*R*,6*R*)
R^{1E} = CH_2OBn, R^{6Z} = OTPS : E,Z-**4h**	**3b**	6	1/99	99	(1*R*,6*R*)
R^{1Z} = CH_2OBn, R^{6Z} = OTPS : Z,Z-**4h**	**3b**	48	99/1	99	(1*S*,6*R*)

[a] Bn = benzyl, TPS = *tert*-butyldiphenylsilyl. The entries with which our results are compared are shown in the frame.

SCHEME 4. Proposed TS for the Major Product in the Claisen Rearrangement Catalyzed by *tert*-Butyl Cu-box

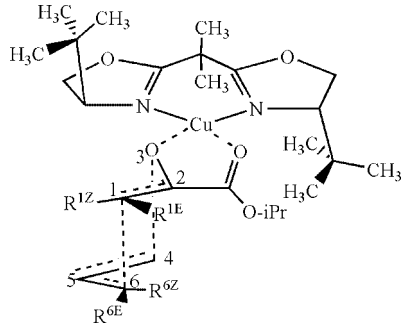

SCHEME 5. Type I Arrangement

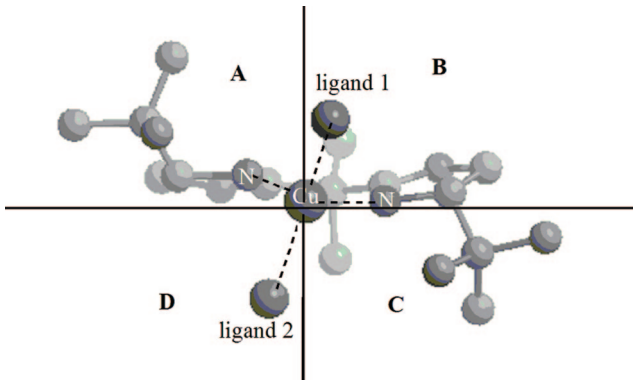

not display a solvent-dependent selectivity.[23,31] Among the recent computational studies of the Cu-box catalyst is one by

SCHEME 6. Type II Arrangement

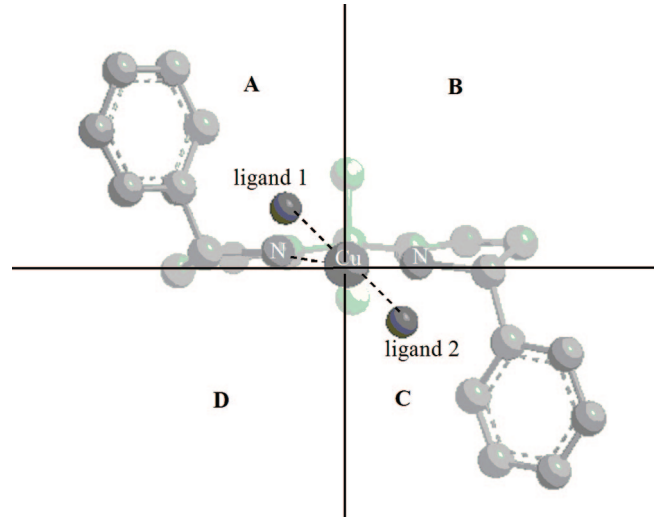

DeChancie et al.[32] that rationalizes the enantioselectivity of the Diels−Alder reactions. The carbonyl-ene reactions have been studied by Morao et al.[33] García and co-workers report on the enantioselectivity of the Cu-box catalysts in the cyclopropanation of alkenes.[34,35]

To the best of our knowledge, there is no computational study on the Cu-box-catalyzed Claisen rearrangement in the literature.

(31) Thorhauge, J.; Roberson, M.; Hazell, R. G.; Jørgensen, K. A. *Chem. Eur. J.* **2002**, *8* (8), 1888–1898.

(32) DeChancie, J.; Acevedo, O.; Evanseck, J. D. *J. Am. Chem. Soc.* **2004**, *126* (19), 6043–6047.

(33) Morao, I.; McNamara, J. P.; Hillier, I. H. *J. Am. Chem. Soc.* **2003**, *125* (3), 628–629.

(34) Fraile, J. M.; García, J. I.; Gil, M. J.; Martínez-Merino, V.; Mayoral, J. A.; Salvatella, L. *Chem. Eur. J.* **2004**, *10* (3), 758–765.

(35) García, J. I.; Jiménez-Osés, G.; Martínez-Merino, V.; Mayoral, J. A.; Pires, E.; Villalba, I. *Chem. Eur. J.* **2007**, *13* (14), 4064–4073.

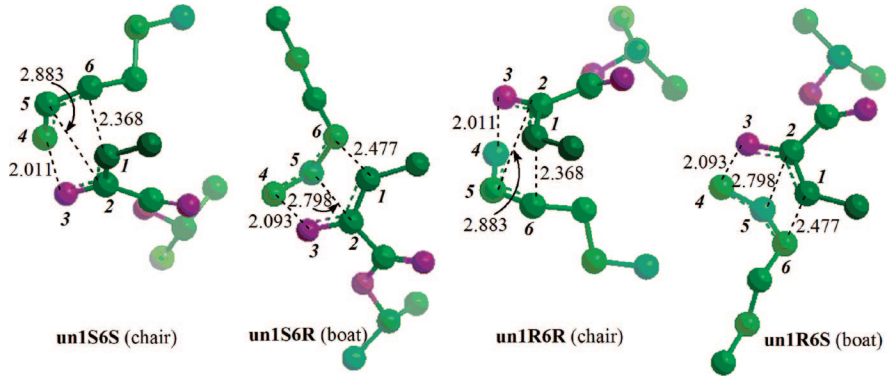

FIGURE 1. Optimized transition structures for the uncatalyzed Claisen rearrangement of *E,Z*-**4a**. Distances in angstroms (green, C; violet, O; hydrogens omitted).

In this work, our aim is to locate the TSs of the *tert*-butyl- or phenyl-substituted Cu-box-catalyzed Claisen rearrangements, as well as that of the uncatalyzed reaction including solvation effects, in order to rationalize the stereochemical outcomes. (*E*,*Z*)-**4a** has been chosen as the substrate because it is known to give high stereoselectivities. X-ray structures show that the OTf^- counterion coordinates to Cu whereas SbF_6^- does not. To save computational time, we have not considered any counterion, assuming that the results should not be too far from the ones in the presence of SbF_6^-. The oxidation state of copper has been taken to be +2 as in the experiments.[3,25,27]

Methods

All stationary point geometries have been optimized at the B3LYP/6-31+G* level of theory[36–39] in the gas phase using the Gaussian03 program.[40] We have computed the harmonic vibrational frequencies for the uncatalyzed reaction, but for the catalyzed reactions we encountered CPHF convergence problems, presumably because of the diffuse functions in the basis set. Therefore, we have reoptimized the structures in the catalyzed reactions using the B3LYP/6-31G* method and computed their harmonic frequencies. Although the lengths of the forming or breaking bonds may differ by 0.08 Å, and the ether O−Cu distance by 0.03 Å between the two basis sets, there is no difference that indicates a change in the nature of the stationary points. Therefore, stationary points in the catalyzed reactions have been characterized at the B3LYP/6-31G* level with local minima having all real frequencies and transition structures having only one imaginary frequency, corresponding to the reaction coordinate. Whether the transition states correspond to the process under consideration is ascertained by animating the transition vectors. Also, thermal and entropic contributions to the Gibbs free energies have been obtained from these frequency calculations.

The geometry optimization for one structure, **ph1S6S**, would only converge when an Ultrafine grid in the numerical DFT calculations was used (B3LYP/6-31+G* level). However, to be consistent with the other structures, a final single point energy evaluation has been carried out using the fine grid, which is the default in Gaussian03.[40]

B3LYP is known to give quite good geometries and ground-state properties but usually underestimates activation barriers and weak interaction energies. We have tested the density functional methods BP86,[36,41] BMK,[42] PBE1PBE,[43,44] MPW1K,[45] and MPWB1K[46] via single point energy calculations using the B3LYP/6-31+G* geometries. The results are given in Tables S1−S3 as Supporting Information. It is known that increasing the amount of the exact exchange in DFT methods leads to an increase in the barrier heights,[45] and our results follow this trend. The functionals that are particularly developed to yield good results for kinetics and that contain high exact exchange (BMK, MPW1K, MPWB1K) give higher (and presumably more realistic) barrier heights. There is a discussion on the choice of the functional and the role of the exact exchange in metal−metal or metal−ligand binding energies in the literature.[47,48] However, in this study, the investigation of the stereoselectivities does not involve any bond formation or dissociation with the metal. The transition states compared with each other can be viewed as different conformers of the same system. Hence, any error coming from the metal−ligand interaction is likely to largely cancel in the study of the stereoselectivities, which is our main concern. Such cancelation is expected to be less marked for the structures that differ more in the environment of the Cu ion. Most TSs display a distorted square planar arrangement around Cu. The structures that deviate more from such planarity are expected to show less error cancelation. Also, the computed activation energies may involve methodological errors. All the tested functionals give quite similar results for selectivities, which are also in reasonable agreement with the experimental observations given in Scheme 3. We have decided to use the MPWB1K/6-31+G* single point results to draw conclusions, because it is known to perform well in describing activation energies and nonbonded

(36) Becke, A. D. *Phys. Rev. A* **1988**, *38* (6), 3098–3103.
(37) Becke, A. D. *J. Chem. Phys.* **1993**, *98* (2), 1372–1377.
(38) Becke, A. D. *J. Chem. Phys.* **1993**, *98* (7), 5648–5652.
(39) Lee, C.; Yang, W.; Parr, R. G. *Phys. Rev. B* **1988**, *37* (2), 785–789.
(40) *Gaussian 03, Revision D.01*; Frisch, M. J.; Trucks, G. W.; Schlegel, H. B.; Scuseria, G. E.; Robb, M. A.; Cheeseman, J. R.; Montgomery, J. A., Jr.; Vreven, T.; Kudin, K. N.; Burant, J. C.; Millam, J. M.; Iyengar, S. S.; Tomasi, J.; Barone, V.; Mennucci, B.; Cossi, M.; Scalmani, G.; Rega, N.; Petersson, G. A.; Nakatsuji, H.; Hada, M.; Ehara, M.; Toyota, K.; Fukuda, R.; Hasegawa, J.; Ishida, M.; Nakajima, T.; Honda, Y.; Kitao, O.; Nakai, H.; Klene, M.; Li, X.; Knox, J. E.; Hratchian, H. P.; Cross, J. B.; Bakken, V.; Adamo, C.; Jaramillo, J.; Gomperts, R.; Stratmann, R. E.; Yazyev, O.; Austin, A. J.; Cammi, R.; Pomelli, C.; Ochterski, J. W.; Ayala, P. Y.; Morokuma, K.; Voth, G. A.; Salvador, P.; Dannenberg, J. J.; Zakrzewski, V. G.; Dapprich, S.; Daniels, A. D.; Strain, M. C.; Farkas, O.; Malick, D. K.; Rabuck, A. D.; Raghavachari, K.; Foresman, J. B.; Ortiz, J. V.; Cui, Q.; Baboul, A. G.; Clifford, S.; Cioslowski, J.; Stefanov, B. B.; Liu, G.; Liashenko, A.; Piskorz, P.; Komaromi, I.; Martin, R. L.; Fox, D. J.; Keith, T.; Al-Laham, M. A.; Peng, C. Y.; Nanayakkara, A.; Challacombe, M.; Gill, P. M. W.; Johnson, B.; Chen, W.; Wong, M. W.; Gonzalez, C.; Pople, J. A.; Gaussian, Inc.: Wallingford, CT, 2004.
(41) Perdew, J. P. *Phys. Rev. B* **1986**, *33* (12), 8822–8824.
(42) Boese, A. D.; Martin, J. M. L. *J. Chem. Phys.* **2004**, *121* (8), 3405–3416.
(43) Perdew, J. P.; Burke, K.; Ernzerhof, M. *Phys. Rev. Lett.* **1996**, *77* (18), 3865–3868.
(44) Perdew, J. P.; Burke, K.; Ernzerhof, M. *Phys. Rev. Lett.* **1997**, *78* (7), 1396.
(45) Lynch, B. J.; Fast, P. L.; Harris, M.; Truhlar, D. G. *J. Phys. Chem. A* **2000**, *104* (21), 4811–4815.
(46) Zhao, Y.; Truhlar, D. G. *J. Phys. Chem. A* **2004**, *108* (33), 6908–6918.
(47) Quintal, M. M.; Karton, A.; Iron, M. A.; Boese, A. D.; Martin, J. M. L. *J. Phys. Chem. A* **2006**, *110* (2), 709–716.
(48) Schultz, N. E.; Zhao, Y.; Truhlar, D. G. *J. Phys. Chem. A* **2005**, *109* (49), 11127–11143.

TABLE 1. Relative Energies (ΔE) and Free Energies (ΔG) of Transition Structures in the Uncatalyzed Reaction and Energy and Free Energy of Activation ($\Delta E^{\ddagger}$ and $\Delta G^{\ddagger}$, Respectively) of the Reaction Computed Using the Lowest Energy Transition Structure[a]

	relative and free energies		
	ΔE_{gas}	$\Delta E_{CH_2Cl_2}$	$\Delta G_{CH_2Cl_2}$
un1S6S	0.0	0.0 (0.0)	0.0
un1R6R	0.0	0.1 (0.1)	0.1
un1S6R	6.0	6.1 (5.6)	5.2
un1R6S	6.0	6.1 (5.7)	5.2
	activation energies		
	$\Delta E^{\ddagger}_{gas}$	$\Delta E^{\ddagger}_{CH_2Cl_2}$	$\Delta G^{\ddagger}_{CH_2Cl_2}$
un1S6S-*E*,*Z*-**4a**	29.9	28.1 (28.7)	29.6

[a] Subscripts gas and CH_2Cl_2 indicate the gas phase and CH_2Cl_2 solution results, respectively. The numbers in parentheses are computed by taking into account only the electrostatic part of the solvation free energy. All values are in kcal/mol.

interactions which are important in determining the selectivities.[49] The systems under consideration in the catalyzed reactions are doublets, whereas the system in the uncatalyzed reaction is closed-shell singlet. Therefore, we used unrestricted and restricted methods for the catalyzed and uncatalyzed reactions, respectively. For the uncatalyzed reaction, we have not considered a biradicaloid TS because the closed-shell B3LYP calculations give better agreement with the experimental activation energy than do the CASSCF calculations, which suggest a biradicaloid electronic structure.[10] Moreover, the more recent kinetic isotope effect measurements by Meyer et al. are in better agreement with the closed-shell B3LYP or MP4 calculations than with the CASSCF results.[7]

We have attempted to optimize all of the geometries using the MPWB1K functional but encountered geometry convergence problems, probably because of a numerical problem discussed by Zhao and Truhlar.[49] Therefore, we have used B3LYP geometries for the MPWB1K single point energy evaluations.

Solvent effects have been taken into account via single point calculations in a dielectric continuum representing CH_2Cl_2 or CH_3CN as the solvent. CH_2Cl_2 is the solvent in which the Cu-box-catalyzed Claisen rearrangement was experimentally studied. The related Diels−Alder reaction was studied in various solvents,[23,31] CH_3CN being the solvent with the largest dielectric constant. CH_3CN is a coordinating solvent for which continuum methods are usually not appropriate. However, in the case of Cu-box-catalyzed Diels−Alder reactions, the substrate displaces the solvent around Cu.[31] We assume that the same phenomenon occurs in the Claisen rearrangement too. Therefore, in the absence of coordination with Cu, the continuum representation of CH_3CN is expected to be appropriate.

The IEFPCM[50–52] continuum method has been used along with the UA0 atomic radii to create the cavity except where indicated. In theory, the free energy (G) of a given structure in the solvent should include the following terms:

$$G = E_{gas} + E_{ZPE+thermal\ gas} + \Delta G_{sol} + \Delta E_{geom} + \Delta E_{ZPE+thermal} \quad (1)$$

where E_{gas} is the gas phase electronic energy (without the zero point energy), $E_{ZPE+thermal\ gas}$ is the sum of the thermal and entropic contributions to the gas phase energy at 298.15 K and the zero point energy (ZPE). ΔG_{sol} is the work required for transferring a system of a given geometry and standard state in vacuum to the solvent. Because it is a work term, ΔG_{sol} corresponds to a free energy and contains not only the energy of solvation but also the thermal and entropic contributions of the solvent to the free energy of solvation, implicitly. ΔE_{geom} is the electronic energy cost of changing the gas phase geometry to the solution phase geometry. $\Delta E_{ZPE+thermal}$ is the difference between gas phase and solution phase ZPE, thermal and entropic contributions of the solute to the free energy. In practice, we have carried out geometry optimizations in the gas phase and assumed that no significant change in geometries occurs in the solvent. Similarly, ZPE, thermal, and entropic contributions to the free energy have been computed only in vacuum. Hence, the last two terms in eq 1 are neglected in free energy calculations.

The electronic energy (E) of the solvated system should contain the energy of solvation added to the gas phase electronic energy. However, continuum calculations yield directly the free energy of solvation. We assume that the thermal and entropic contributions of the solvent to ΔG_{sol} are more or less similar among different structures and hence, cancel out when computing the relative energies (ΔE) which are the values discussed in this paper. Therefore, the electronic energies in solution are evaluated according to

$$E = E_{gas} + \Delta G_{sol} \quad (2)$$

To analyze the solvent effects in more detail, we divide the solvation free energy (ΔG_{sol}) into an electrostatic (ΔG_{sol}^{el}) and a nonelectrostatic component ($\Delta G_{sol}^{non\ el}$), the former being computed quantum mechanically, whereas $\Delta G_{sol}^{non\ el}$ is calculated empirically:

$$\Delta G_{sol}^{non\ el} = \Delta G_{sol}^{cav} + \Delta G_{sol}^{rep} + \Delta G_{sol}^{disp} \quad (3)$$

where ΔG_{sol}^{cav} is the energy required to form a cavity of the size of the solute in the bulk solvent (cavitation energy), ΔG_{sol}^{rep} is the repulsion energy between the solute and the solvent, and ΔG_{sol}^{disp} is the solute−solvent dispersion energy. The effect of the solvent polarity on the solute−solvent interactions is contained in ΔG_{sol}^{el}. In order to show the effect of electrostatic solvation more clearly, the relative energies computed by taking into account only ΔG_{sol}^{el} are given in parentheses in the tables. Individual ΔG_{sol}^{el} and $\Delta G_{sol}^{non\ el}$values in CH_2Cl_2 are given as Supporting Information in Table S4. However, it should be borne in mind that continuum models are not generally accurate to a few tenths of a kilocalorie and hence should be used to predict trends rather than absolute values.

In the uncatalyzed reaction, the activation free energy is calculated with respect to the most stable conformer of the reactant, whereas in the catalyzed reactions, it is calculated with respect to the most stable conformer of the substrate−catalyst complex.

Results and Discussion

Uncatalyzed Reaction. Geometries of the four transition states leading to the four different stereoisomers are shown in Figure 1. Relative energies and activation energies are given in Table 1. Cartesian coordinates of all the TSs and the reactant are given as Supporting Information. The structures are named according to the stereochemistry of the related products at the carbon atoms 1 and 6, along with the prefix **un**, standing for uncatalyzed.

The lowest energy transition states are **un1S6S** and **un1R6R**, which display chair-like structures, as expected. Because of the steric repulsion between C2 and C5 atoms, the boat-like TSs **un1R6S** and **un1S6R** are higher in free energy by 5 kcal/mol, in agreement with the high diastereoselectivity of the Claisen rearrangements. This steric effect is also reflected in the lengths

(49) Zhao, Y.; Truhlar, D. G. *J. Chem. Theory Comput.* **2005**, *1* (3), 415–432.
(50) Cancès, E.; Mennucci, B.; Tomasi, J. *J. Chem. Phys.* **1997**, *107* (8), 3032–3041.
(51) Mennucci, B.; Cancès, E.; Tomasi, J. *J. Phys. Chem. B* **1997**, *101* (49), 10506–10517.
(52) Cancès, E.; Mennucci, B. *J. Math. Chem.* **1998**, *23* (3−4), 309–326.

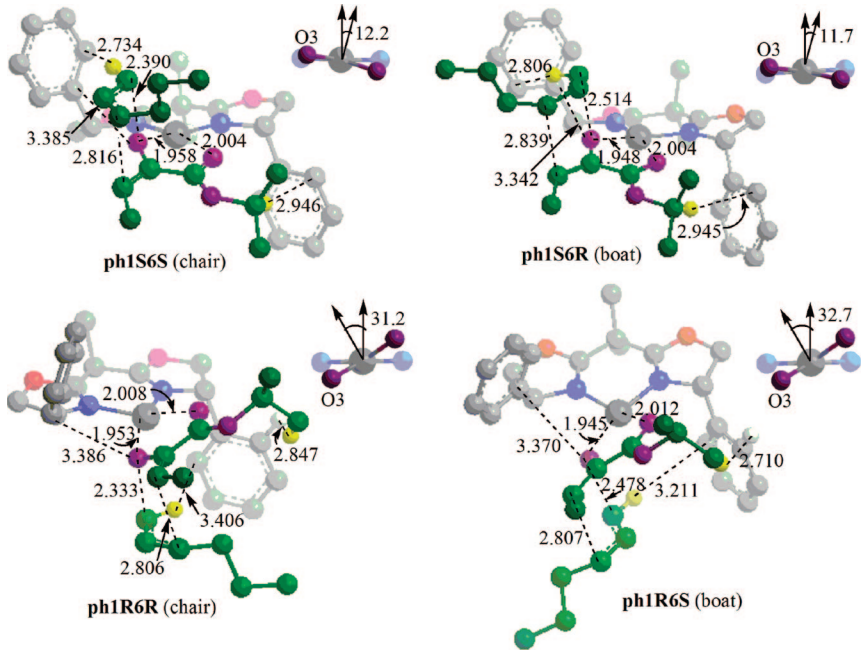

FIGURE 2. Transition structures for the phenyl Cu-box-catalyzed Claisen rearrangement of *E,Z*-**4a** (green, substrate C; yellow, substrate H; violet, substrate O; grey, catalyst C; white, catalyst H; red, catalyst O; blue, N; dark grey, Cu). Some hydrogens are omitted. The angles between the normal vectors to the O−Cu−O and N−Cu−N planes are also shown. Distances in angstroms, angles in degrees.

of the forming and breaking bonds, which are longer by 0.08−0.11 Å in boat-like TSs than in chair-like TSs. For all TSs the breaking bond distances are shorter than the forming bond distances by 0.36−0.39 Å. Enantiomeric TSs have identical energies in the gas phase as expected. However, due to numerical errors in the solution phase calculations a 0.1 kcal/mol energy difference between **un1S6S** and **un1R6R** has been found. This value has no physical significance and comes entirely from a computational artifact.

The free energy of activation (29.6 kcal/mol) has been computed with respect to the lowest energy TS **un1S6S** and the most stable conformer of the reactant (not shown). Similar values of the free energy of activation are commonly observed in Claisen rearrangements.[53,54]

The effect of the solvent on the relative energies of the TSs is at most 0.1 kcal/mol. The decrease in $\Delta E^{\ddagger}$ upon solvation is 1.8 kcal/mol. We have checked whether the atomic radii used to create the solute−cavity have any effect on the computed activation energy. We have carried out single point energy calculations using some of the standard radii avalaible in Gaussian03. The $\Delta E^{\ddagger}_{CH_2Cl_2}$ value is 29.8 (28.2), 30.6 (28.9), 28.7 (28.7), and 28.1 (28.7) kcal/mol, respectively, for the Bondi, UAHF, UFF and UA0 radii, the numbers in parentheses being the values computed taking into account only the electrostatic part of the solvation energy. These results suggest a small decrease in the barrier height due to electrostatic solvation effects. However, the nonelectrostatic part of the solvent effect is not consistent between different radii, the overall $\Delta E^{\ddagger}_{CH_2Cl_2}$ value being either similar (Bondi), higher (UAHF), or lower than $\Delta E^{\ddagger}_{gas}$ (UFF, UA0). In all cases, the effect of the solvent on the barrier height is small and we thus find that the reaction is not very sensitive to solvent effects.

(53) Schuler, F. W.; Murphy, G. W. *J. Am. Chem. Soc.* **1950**, *72* (7), 3155–3159.

(54) Burrows, C. J.; Carpenter, B. K. *J. Am. Chem. Soc.* **1981**, *103* (23), 6983–6984.

TABLE 2. Relative Energies (ΔE) and Free Energies (ΔG) of Transition Structures in the Reaction Catalyzed by phenyl Cu-box and Energy and Free Energy of Activation ($\Delta E^{\ddagger}$ and $\Delta G^{\ddagger}$, Respectively) of the Reaction Computed Using the Lowest Energy Transition Structure[a]

	relative and free energies			
	ΔE_{gas}	$\Delta E_{CH_2Cl_2}$	ΔE_{CH_3CN}	$\Delta G_{CH_2Cl_2}$
ph1S6S	0.0	0.0 (0.0)	0.0 (0.0)	0.0
ph1S6R	1.1	2.6 (1.8)	2.7 (1.8)	2.6
ph1R6R	−0.5	3.6 (0.3)	4.0 (0.4)	3.5
ph1R6S	1.0	6.7 (3.1)	7.5 (3.5)	6.8
	activation energies			
	$\Delta E^{\ddagger}_{gas}$	$\Delta E^{\ddagger}_{CH_2Cl_2}$	$\Delta E^{\ddagger}_{CH_3CN}$	$\Delta G^{\ddagger}_{CH_2Cl_2}$
ph1S6S-rph1S6R	16.6	15.0 (16.7)	15.3 (17.1)	13.8
ph1R6R-rphext	18.4			

[a] Subscripts gas, CH_2Cl_2, and CH_3CN indicate the reaction medium. The numbers in parentheses are computed by taking into account only the electrostatic part of the solvation free energy. All values are in kcal/mol.

Phenyl-Substituted Cu-box Catalyzed Reaction. Transition structure searches starting with various substrate−catalyst orientations have yielded four TSs. The optimized geometries of these TSs are displayed in Figure 2. Relative energies and activation energies are given in Table 2. Cartesian coordinates of all the TSs and related reactants are given as Supporting Information. The structures are named according to the stereochemistry of the related products at the carbon atoms 1 and 6, along with the prefix **ph**, standing for phenyl. The prefix **r** indicates a reactant complex. An extended conformer of the reactant complex is named **rphext**.

There are a number of common properties for all the structures. First, in all TSs in the catalyzed reaction, the distances between the allyl and enolate moieties, i.e., the forming and breaking bonds, are longer than the corresponding distances in the uncatalyzed reaction by 0.3−0.5 Å. Apparently, the Lewis

acid attracts part of the electron density of the substrate, weakening the forming and breaking bonds in the TSs.

Second, the isopropyl ester part displays a different conformation than in the uncatalyzed reaction. In the presence of the catalyst, the carbonyl O is oriented toward Cu and is cis to the ether O, while the isopropyl group stays away from box, avoiding steric interactions.

Structures **ph1S6S** and **ph1S6R** exhibit a type II arrangement, whereas **ph1R6R** and **ph1R6S** show a type I orientation. In **ph1R6R** and **ph1R6S**, the isopropyl ester part is situated in quadrant B, while the vinyl part is in quadrant D. This arrangement leaves enough space for the allyl part in quadrants C and D, minimizing steric interactions (Figure 2). For instance, the closest H−H contacts between the substrate and the catalyst are 2.710−2.847 Å. These contacts involve a hydrogen on the isopropyl group and a hydrogen on the phenyl group in quadrant C. The distance between the hydrogen on C4 and the closest carbon atom of the phenyl group in quadrant C is also large (3.211−3.406 Å). A possible unfavorable interaction can occur between O3 carrying a partial negative charge and the delocalized electron cloud of the phenyl group in quadrant A. The shortest distance between O3 and a phenyl C is 3.370−3.386 Å, slightly larger than the sum of their van der Waals radii.

Because the phenyl group is planar and is not too bulky, it may adapt its conformation according to its environment. Hence, in **ph1S6S** and **ph1S6R**, the isopropyl group of the substrate can be situated in the same quadrant as one of the phenyl groups without significant steric interactions (Figure 2). For instance, the shortest distance between an isopropyl H and a phenyl carbon in quadrant C is 2.945−2.946 Å. However, if the substrate had a more branched group such as *tert*-butyl in the ester part, there would probably not be enough room for it in quadrant C. Therefore, **ph1S6S** and **ph1S6R** would be highly destabilized. Conversely, the replacement of the isopropyl group by -CH_3 would not provide an important stabilization of **ph1S6S** and **ph1S6R**, because the terminal C atoms of the isopropyl are already oriented away from the catalyst. Therefore, the interaction of the isopropyl with phenyl would be practically the same as that of the methyl, in agreement with experiment.[3] On the other hand, the distance between O3 and the closest C of the phenyl group in quadrant A is similar as in the type I structures (3.342−3.385 Å). The hydrogen on C4 makes close contacts with the phenyl group (2.734−2.806 Å). It is not clear whether this interaction is repulsive or a T-shaped π-stacking type attractive interaction. For instance, NBO[55,56] calculations yield a charge transfer energy of 1.8 kcal/mol between phenyl and allyl in **ph1S6S**. The charge transfer energy between allyl and phenyl in **ph1R6R** is negligible (0.1 kcal/mol).

To sum up, in any TS the isopropyl group is not involved in important steric interactions. The O3-phenyl distances are similar in all TSs, but, since O3 is in the direction of the p orbitals of the phenyl group in type II TSs, the repulsive interactions may be slightly more important. This may be partially compensated by the T-shaped attractive interactions between the C4 hydrogen and phenyl (if any). As a result, enantiomeric TSs have very similar energies in the gas phase, the type II ones being slightly higher in energy than the enatiomeric type I, resulting in low enantioselectivity.

Since **ph1S6R** and **ph1R6S** display boat-like structures, they are less stable by 1.1 and 1.5 kcal/mol than the chair-like **ph1S6S** and **ph1R6R**, respectively, in the gas phase. These values are surprisingly low compared to the chair-TS/boat-TS energy difference in the uncatalyzed reaction. The differences in the substrate-Cu or substrate-box interaction distances among the TSs do not seem to be responsible for the decrease in the chair-boat TS energy difference (Figure 2). For instance, the O3−Cu distances differ by only 0.01 Å among diastereomeric TSs. The isopropyl H-phenyl C or O3-phenyl C distance are also very similar. Apparently, because the vinyl and allyl moieties are farther away from each other in the presence of the catalyst with respect to the uncatalyzed reaction, the steric repulsion between C2 and C5 is less important. For instance, the C2−C5 distance is 2.999 Å in both **ph1S6R** and **ph1R6S**. As a result, **ph1R6S** and **ph1S6R** have low ΔE values for boat-like TSs.

In Figure 2, the angles between the vectors normal to the O−Cu−O and N−Cu−N planes are displayed. In a perfect square planar arrangement these angles should be 0°, whereas in a perfect tetrahedral arrangement they should be 90°. Thus, all the TSs in Figure 2 show a distorted square planar arrangement rather than a tetrahedral one. The distortion is larger in the type I structures.

Both the enantioselectivity and diastereoselectivity are solvent dependent. In going from vacuum to CH_2Cl_2, the energy difference between the TSs yielding enantiomeric products changes by about 4 kcal/mol in favor of **ph1S6S** and **ph1S6R** with respect to **ph1R6R** and **ph1R6S**, respectively. Also, the energy difference between the TSs yielding diastereomeric products changes by about 1.5 kcal/mol in favor of **ph1S6S** and **ph1R6R** with respect to **ph1S6R** and **ph1R6S**, respectively. In the gas phase, **ph1R6R** is slightly lower in energy than **ph1S6S**, but in CH_2Cl_2, **ph1S6S** becomes the lowest energy TS. The more polar solvent CH_3CN has little effect on the selectivity and this effect is in the same direction as that of CH_2Cl_2.

To make sure that the solvent dependence of the stereoselectivity with phenyl Cu-box does not originate from a computational artifact, we have computed the relative energy of **ph1R6R** with respect to **ph1S6S** in the gas phase and in CH_2Cl_2 using various DFT functionals. The ΔE_{gas} values are −2.0, −1.9, −1.5, 0.4, −1.7, and −0.5 kcal/mol for the BP86, B3LYP, PBE1PBE, BMK, MPW1K, and MPWB1K functionals, respectively. The corresponding $\Delta E_{CH_2Cl_2}$ values are 1.8 (−1.5), 2.1 (−1.2), 2.5 (−0.8), 4.4 (1.1), 2.5 (−0.9), and 3.6 (0.3) kcal/mol, the numbers in parentheses being the values computed by taking into account only the electrostatic part of the solvation energy. Moreover, in order to see the effect of the radii of the spheres used to create the solute−cavity in the solvent, we have computed $\Delta E_{CH_2Cl_2}$ using some of the standard radii available in Gaussian03 in combination with the MPWB1K method. The $\Delta E_{CH_2Cl_2}$ values are 3.2 (1.5), 4.0 (3.0), 3.7 (0.6), 1.5 (−0.1), and 3.6 (0.3) using the Bondi, Pauling, UFF, UAHF, and UA0 radii, respectively. In the gas phase all methods except BMK predict that **ph1R6R** is the lowest energy TS. On the other hand, in CH_2Cl_2, calculations with all methods and all radii find **ph1S6S** as the lowest energy TS. However, the quantitative results and the relative importance of the electrostatic and nonelectrostatic parts of the solvent effects are different. If only the electrostatic solvent effects are considered, BP86, B3LYP, PBE1PBE, and MPW1K along with the UA0

(55) Reed, A. E.; Curtiss, L. A.; Weinhold, F. *Chem. Rev.* **1988**, *88* (6), 899–926.
(56) Reed, A. E.; Weinstock, R. B.; Weinhold, F. *J. Chem. Phys.* **1985**, *83* (2), 735–746.

radii, and MPWB1K with the UAHF radii predict that **ph1R6R** is lower in energy than **ph1S6S**. Nevertheless, in all these cases $\Delta E_{CH_2Cl_2}$ (see the numbers in parentheses) is less negative than ΔE_{gas}, indicating that solvation of electrostatic nature favors **ph1S6S** with respect to **ph1R6R**. Also, the non electrostatic solvent effects favor **ph1S6S**, yielding positive $\Delta E_{CH_2Cl_2}$ values. Since $\Delta G_{sol}^{non\ el}$ is computed empirically, it may yield unreliable results as in the uncatalyzed reaction above. Nevertheless, the more favorable nonelectrostatic solvation energy for **ph1S6S** can be rationalized in part by considering the geometries of **ph1S6S** and **ph1R6R**. Since the substrate and the substituents of the catalyst are situated in the same quadrants of the space, **ph1S6S** is more compact (the cavity volume is 905.410 and 938.164 Å^3 for **ph1S6S** and **ph1R6R**, respectively). Hence, less energy is required to create a cavity in the solvent. Indeed, ΔG_{sol}^{cav} is 55.7 and 58.1 kcal/mol for **ph1S6S** and **ph1R6R**, respectively (MPWB1K/UA0). The other contributions to $\Delta G_{sol}^{non\ el}$ exhibit smaller variations between these structures (ΔG_{sol}^{rep} is 1.6 and 1.5 kcal/mol, ΔG_{sol}^{disp} is −32.8 and −31.8 kcal/mol for **ph1S6S** and **ph1R6R**, respectively). Thus, although we do not expect to obtain quantitatively accurate results for the large systems studied here using DFT and continuum methods, we are confident that the stereoselectivity of the Claisen rearrangement with the phenyl Cu-box is solvent dependent and that both the electrostatic and nonelectrostatic parts of the solvent effect favor **ph1S6S**. The experimental observations for *E*,*Z*-**4a** (Scheme 3),[3,25,27] which is the system studied in this work, are in reasonable agreement with our computational results in CH_2Cl_2.

It is not only the lowest energy TS but also the most stable reactant complex that is different in the solvent (**rph1S6R**) compared to the vacuum state (**rphext**). The activation energies in Table 2 are computed as the energy difference between the lowest energy TS and the most stable reactant complex in each medium. Thus, $\Delta E^{\ddagger}_{gas}$ is the energy difference between **ph1R6R** and **rphext** while $\Delta E^{\ddagger}_{CH_2Cl_2}$ and $\Delta E^{\ddagger}_{CH_3CN}$ refer to the energy difference between **ph1S6S** and **rph1S6R**. It is useful to compare the solution phase activation energies, i.e., the energy difference between **ph1S6S** and **rph1S6R** in CH_2Cl_2 or CH_3CN, with the gas phase energy difference between **ph1S6S** and **rph1S6R**, in order to monitor the solvent effects on this value. Therefore, the gas phase energy difference between **ph1S6S** and **rph1S6R** is also included in Table 2, although it does not correspond to the gas phase activation energy. The $\Delta G^{\ddagger}$ value of 13.8 kcal/mol in CH_2Cl_2 seems to be somewhat smaller than expected considering the experimental completion times[3,25,27] probably because of the omission of the counterions. The activation energy decreases in going from vacuum to CH_2Cl_2, then slightly increases in CH_3CN with respect to the one in CH_2Cl_2. If only the electrostatic part of the solvation energy is considered, an insignificant increase in the barrier height (computed as the **ph1S6S**-**rph1S6R** energy difference in all three media) with increasing dielectric constant is observed. Thus, we conclude that the reaction rate is insensitive to the dielectric constant.

It is interesting to compare the $-T\Delta S^{\ddagger}$ term in the uncatalyzed (3.0 kcal/mol) and catalyzed reactions (0.6 kcal/mol). Note that this term includes only the solute entropy in our calculations. The small value for the catalyzed reaction suggests that the motion of the reactant state is already quite restricted in the presence of the catalyst and not too much entropy loss takes place in going to the transition state.

***tert*-Butyl-Substituted Cu-box Catalyzed Reaction.** The optimized geometries of the transition states for the *tert*-butyl-substituted Cu-box catalyzed reaction leading to the different stereoisomers are shown in Figure 3. Relative energies and activation energies are given in Table 3. Unlike the phenyl-substituted Cu-box, two different TSs have been located for each of the (1*S*,6*S*) and (1*S*,6*R*) stereoisomers. The structures are named according to the stereochemistry of the related products at the carbon atoms 1 and 6, along with the prefix **tb**, standing for *tert*-butyl. In the case of **tb1S6S** and **tb1S6R**, the two TSs are differentiated by suffices **a** or **b**. The prefix **r** denotes a reactant complex. Cartesian coordinates of all the TSs and related reactants are given as Supporting Information. The reactant complex corresponding to **tb1S6Sa** collapses to **rtb1R6S** upon optimization.

The *tert*-butyl group is bulkier than the phenyl group and in addition because of its C_{3v} local symmetry, it cannot assume various conformations to accommodate a given conformation of the substrate. Therefore, only in **tb1R6R** and **tb1R6S** can large steric interactions between box and the substrate be avoided (Figure 3). Even in these structures, there are short H−H contact distances in quadrant C (2.386−2.460 Å). Both structures display a type I arrangement, putting the allyl moiety in quadrants C and D, away from the catalyst. Among these two structures, **tb1R6R** is of lower energy due to the chair-like shape of the substrate. As in the case of the phenyl Cu-box, the boat-like TS **tb1R6S** is not too high in energy with respect to **tb1R6R**, because of the relatively large distance between the enolate and allyl moieties, leading to decreasing the steric interactions between them.

Species **tb1S6Sa** and **tb1S6Ra** also have type I arrangements. However, in these structures the allyl part is located in quadrant D, putting the allylic protons at C4 in close contacts with the catalyst (Figure 3). Short H−H contact distances of 2.2 Å occur in quadrant D. If the substrate rotates counter clockwise to remove these interactions, then the isopropyl ester and vinyl groups intrude into quadrants A and C, respectively, making close contacts with the catalyst. Steric interactions also push the substrate away from the catalyst as shown by the Cu−O distances (Figure 3). The boat-like TS **tb1S6Ra** has a higher energy than **tb1S6Sa**.

Structures **tb1S6Sb** and **tb1S6Rb** exhibit type II arrangements. However, because the allyl part and a *tert*-butyl group cannot be accommodated in quadrant A, and the isopropyl group and the other *tert*-butyl in quadrant C, without large steric contacts, the plane of the catalyst bends. As such, in **tb1S6Sb**, the unfavorable interaction distances are larger than in **tb1S6Sa**. This bending of the catalyst has an energy cost. These two effects together render **tb1S6Sb** lower in energy than **tb1S6Sa**. On the other hand, in **tb1S6Rb**, even the bending of the catalyst is not enough to remove the steric interactions. For example, a proton on C4 is situated at a distance of 2.239 Å from a proton of the *tert*-butyl group in quadrant A (Figure 3).

Structures **tb1R6R** and **tb1R6S** display distorted square planar geometries around Cu as shown by the angles given in Figure 3. The extent of the distortion is similar as the type I TSs in the phenyl Cu-box catalyzed reaction. Structures **tb1S6Sa** and **tb1S6Ra** display larger deviations from square planarity because of the large steric interactions involving the allyl moiety in quadrant D; they are between a square planar and a tetrahedral geometry. The bending of the catalyst in **tb1S6Sb** and **tb1S6Rb** does not involve the coordination of Cu. These two type II TSs

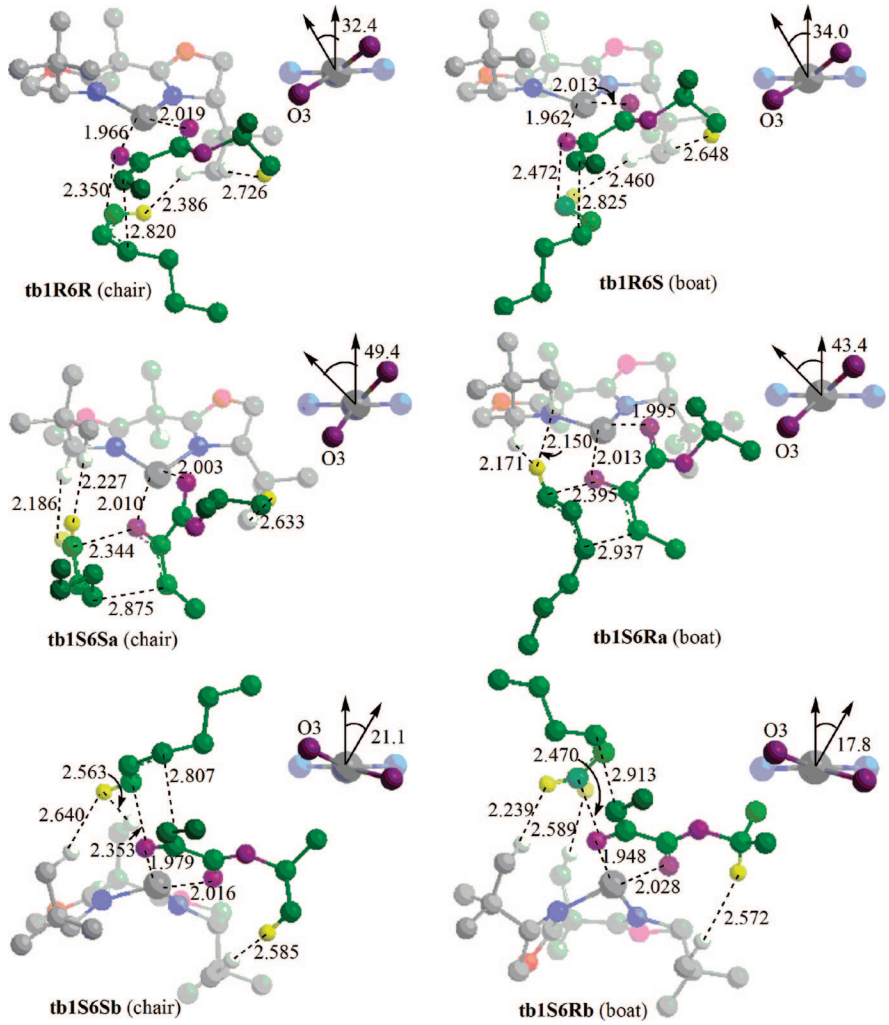

FIGURE 3. Transition structures for the *tert*-butyl Cu-box catalyzed Claisen rearrangement of *E*,*Z*-**4a** (green, substrate C; yellow, substrate H; violet, substrate O; grey, catalyst C; white, catalyst H; red, catalyst O; blue, N; dark grey, Cu). Some hydrogens are omitted. The angles between the normal vectors to the O−Cu−O and N−Cu−N planes are also shown. Distances in angstroms, angles in degrees.

TABLE 3. Relative Energies (Δ*E*) and Free Energies (Δ*G*) of Transition Structures in the Reaction Catalyzed by *tert*-Butyl Cu-box and Energy and Free Energy of Activation (Δ$E^{‡}$ and Δ$G^{‡}$, Respectively) of the Reaction Computed Using the Lowest Energy Transition Structure[a]

	relative and free energies			
	ΔE_{gas}	$\Delta E_{CH_2Cl_2}$	ΔE_{CH_3CN}	$\Delta G_{CH_2Cl_2}$
tb1R6R	0.0	0.0 (0.0)	0.0 (0.0)	0.0
tb1R6S	1.1	1.4 (1.8)	1.6 (1.8)	1.3
tb1S6Sa	7.4	6.9 (7.7)	7.3 (8.2)	6.5
tb1S6Sb	6.9	6.7 (6.5)	6.6 (6.4)	5.8
tb1S6Ra	7.8	7.6 (8.5)	8.1 (9.0)	7.4
tb1S6Rb	9.9	11.4 (10.4)	12.2 (10.8)	9.7
	activation energies			
	$\Delta E^{‡}_{gas}$	$\Delta E^{‡}_{CH_2Cl_2}$	$\Delta E^{‡}_{CH_3CN}$	$\Delta G^{‡}_{CH_2Cl_2}$
tb1R6R-rtb1R6S	19.2	18.4 (17.9)	18.1 (17.7)	17.4

[a] Subscripts gas, CH_2Cl_2 and CH_3CN indicate the reaction medium. The numbers in parentheses are computed by taking into account only the electrostatic part of the solvation free energy. All values are in kcal/mol.

show small deviations from square planarity, not too far from the deviations in **ph1S6S** and **ph1S6R**, the type II TSs in the phenyl Cu-box catalyzed reaction.

Solvent effects do not change the order of relative energies. Neither the enantioselectivity, nor the diastereoselectivity is very sensitive to the solvation effects. The diasteroselectivity is expected to increase only slightly with increasing polarity of the solvent whereas the decrease in the relative energy of **tb1S6Sb** leads to a very small decrease in the enantioselectivity. Note, however, that the relative energy of **tb1S6Sb** is still too large.

Some experimental results using *tert*-butyl Cu-box along with SbF_6^- as counterion and CH_2Cl_2 as the solvent are summarized in Scheme 3.[27] Our results are in agreement with experiments in that **tb1R6R** is the lowest energy TS for *E*,*Z*-**4a**.

The activation free energy has been computed as the free energy difference between **tb1R6R** and the most stable reactant complex which is the precursor of **tb1R6S** (not shown). The Δ$G^{‡}$ value of 17.4 kcal/mol seems to be somewhat smaller than expected for a reaction with a completion time of 3 h, probably because of the omission of the counterions. The activation free energy with *tert*-butyl Cu-box is higher than with phenyl Cu-box. The activation energy with *tert*-butyl Cu-box decreases only slightly in going from vacuum to CH_2Cl_2 then to CH_3CN.

The $-T\Delta S^{‡}$ term is again much smaller (0.8 kcal/mol) for the catalyzed reaction than for the uncatalyzed reaction (3.0 kcal/mol). Thus, in the *tert*-butyl Cu-box, as in phenyl Cu-box, the

motion of the reactant state is already quite restricted and part of the catalytic effect comes from the reduction of the activation entropy.

Solvent Effects. In Table S4, three trends can be observed. First, the structures with a chair-like TS are better solvated electrostatically with respect to the boat-like TSs, leading to the corresponding diastereomeric products, except the ones involved in the uncatalyzed reaction. This is also true for the corresponding conformers of the reactant complexes. Second, type II structures have more negative ΔG_{sol}^{el} values as compared with type I structures yielding the corresponding enantiomeric products (**rtb1S6Sb** is an exception). Third, in general, the TSs are better solvated electrostatically than the corresponding reactant complexes with the exception of **ph1S6S** and **ph1S6R**. The small differences in ΔG_{sol}^{el} values make it difficult to attribute the observed trends to a particular reason.

Conclusion

Phenyl- and *tert*-butyl-substituted Cu-box catalyzed Claisen rearrangement reactions of *E*,*Z*-**4a** as well as the uncatalyzed reaction have been studied computationally. Reaction with phenyl Cu-box has a low enantioselectivity and diastereoselectivity in the gas phase, giving (1*R*,6*R*) as the major product. The phenyl group is not too bulky and can adapt its conformation to that of the substrate. Therefore, two different arrangements, called type I and type II here, are energetically close to each other in the gas phase. Moreover, the distance between the enolate and allyl moieties in the TS is relatively large, reducing the steric repulsions in boat-like TSs. The low degree of steric interactions between the substrate and the catalyst as well as between different parts of the substrate is responsible for the low selectivity in vacuum. The CH_2Cl_2 solvent induces a good level of selectivity and a reversal of the absolute configuration (1*S*,6*S*). On the other hand, with the bulkier *tert*-butyl group, only **tb1R6R** and **tb1R6S** can avoid large steric interactions between the substrate and box. Among these two structures, the chair-like one, **tb1R6R**, is the lowest energy one both in the gas phase and in CH_2Cl_2.

To our knowledge, Cu-box catalyzed Claisen rearrangements were studied experimentally only in CH_2Cl_2. Therefore, experiments in different media are required to validate our computational predictions concerning the impact of the solvent on the stereoselectivity. On the other hand, solvent effects on the Cu-box catalyzed Diels−Alder reactions were studied and it was found that the selectivity with phenyl Cu-box is very sensitive to the solvent dielectric constant.[23,31] However, in these experiments, it was observed that at low dielectric, phenyl Cu-box gives the opposite absolute configuration with respect to *tert*-butyl Cu-box, whereas at high dielectric, it gives the same absolute configuration. In our work, we find that in vacuum (i.e., at the lowest limit of the dielectric) both catalysts yield the same absolute configuration whereas with increasing dielectric, the selectivity is reversed. An explanation for the different behavior of Claisen and Diels−Alder reactions needs further studies.

The investigation of the electrostatic part of the solvent effects indicates three trends (Table S4, Supporting Information): (i) chair-like TSs are better solvated than the boat-like TSs yielding the corresponding diastereomeric product (except in the uncatalyzed reaction), (ii) type II structures are favored by the solvent with respect to the type I TSs leading to the enantiomeric products (**rtb1S6Sb** is an exception), and (iii) the TSs are better solvated electrostatically than the corresponding reactant complexes with the exception of **ph1S6S** and **ph1S6R**.

The $-T\Delta S^{\ddagger}$ term in the presence of the catalyst is much smaller than the one in the uncatalyzed reaction. Hence, part of the catalytic action of Cu-box comes from the entropic effects.

Although our work is concerned only with *E*,*Z*-**4a**, it gives insight about other experimentally studied systems. For example, Z,Z-**4a** is expected to pass through TSs like **ph1S6S** or **tb1R6R** in order to give the observed selectivity with the phenyl or *tert*-butyl Cu-box, respectively (Scheme 3).[3,25,27] Considering the optimized geometries of **ph1S6S** and **tb1R6R** it can be said that putting the methyl group at the Z position would not yield any new interaction that might change the basic features of the TSs. On the other hand, experiments indicate a competiton between chair and boat-like TSs for E-configured allyl groups.[3,25,27] Our calculations show that the boat-chair TS energy difference is greatly reduced in the presence of the catalyst, making the competition between them possible. However, the reason why the competition happens particularly in systems with E-configured allyl groups requires further study.

Acknowledgment. This research was supported by the British Council and Boğaziçi University Research Grant, BAP (Project No. 06HB505). Computational resources were also provided by TUBITAK ULAKBIM High Performance Computing Center and the University of Manchester. C.Ö. and B.B. acknowledge the sixth framework project COSBIOM (FP6-2004-ACC-SSA-2, Project No 517991).

Supporting Information Available: Tables S1−4, Cartesian coordinates and energies (in various media) of all structures. This material is available free of charge via the Internet at http://pubs.acs.org.

JO800101G